Article

Floating Photovoltaic Systems Coupled with Pumped Hydroplants under Day-Ahead Electricity Market Conditions: Parametric Analysis

Arsenio Barbón [1], **Javier Aparicio-Bermejo** [2], **Luis Bayón** [3,*] **and Ramy Georgious** [1]

1 Department of Electrical Engineering, University of Oviedo, 33003 Oviedo, Spain; barbon@uniovi.es (A.B.); georgiousramy@uniovi.es (R.G.)
2 Business Development Iberia Northwest Area, Enel Green Power, 28014 Madrid, Spain; javierapariciobermejo@gmail.com
3 Department of Mathematics, University of Oviedo, 33003 Oviedo, Spain
* Correspondence: bayon@uniovi.es

Abstract: The intermittent nature of the solar resource together with the fluctuating energy demand of the day-ahead electricity market requires the use of efficient long-term energy storage systems. The pumped hydroelectric storage (*PHS*) power plant has demonstrated its technical and commercial viability as a large-scale energy storage technology. The objective of this paper is to analyse the parameters that influence the mode of operation in conjunction with a floating photovoltaic (*FPV*) power plant under day-ahead electricity market conditions. This work proposes the analysis of two parameters: the size of the *FPV* power plant and the total process efficiency of the *PHS* power plant. Five *FPV* plant sizes are analysed: 50% (*S1*), 100% (*S2*), 150% (*S3*), 350% (*S4*) and 450% (*S5*) of the *PHS* plant. The values of the total process efficiency parameter analysed are as follows: 0.77 for old *PHS* plants, and 0.85 for more modern plants. The number of daily operating hours of the *PHS* plant is 4 h. These 4 h of operation correspond to the highest prices on the electricity market. The framework of the study is the Iberian electricity market and the Alto Rabagão dam (Portugal). Different operating scenarios are considered to identify the optimal size of the *FPV* power plant. Based on the measured data on climatic conditions, an algorithm is designed to estimate the energy production for different sizes of *FPV* plants. If the total process efficiency is 0.85, the joint operation of both plants with *FPV* plant sizes *S2* and *S3* yields a slightly higher economic benefit than the independent mode of operation. If the total process efficiency is 0.77, there is always a higher economic benefit in the independent operation mode, irrespective of the size of the *FPV* plant. However, the uncertainty of the solar resource estimation can lead to a higher economic benefit in the joint operation mode. Increasing the number of operating hours of the *PHS* plant above 4 h per day decreases the economic benefit of the joint operation mode, regardless of the total process efficiency parameter and the size of the *FPV* plant. As the number of operating hours increases, the economic benefit decreases. The results obtained reveal that the coupling of floating photovoltaic systems with pumped hydroelectric storage power plants is a cost-effective and reliable alternative to provide sustainable energy supply security under electricity market conditions. In summary, the purpose of this work is to facilitate decision making on the mode of operation of both power plants under electricity market conditions. The case studies allow to find the optimal answer to the following practical questions: What size does the *FPV* power plant have to be in order for both plants to be better adapted to the electricity market? What is the appropriate mode of operation of both plants? What is the economic benefit of changing the turbine pump of the *PHS* power plant? Finally, how does the installation of the *FPV* power plant affect the water volume of the upper reservoir of the *PHS* plant? Knowledge of these questions will facilitate the design of *FPV* power plants and the joint operation of both plants.

Keywords: pumped hydroelectric storage power plant; floating photovoltaic power plant; day-ahead market; economic benefits

1. Introduction

Limiting global average temperature increases to 1.5 ($°$C) above pre-industrial levels in accordance with the Paris Agreement [1] is a goal for most governments. To achieve this, CO_2 emissions must be reduced to net zero by 2050 as far as possible [2]. In this sense, the European Union (*EU*) has set decarbonisation strategies for 2030, which can be summarised by means of the objectives set out in the Winter Package [3]: (i) a 40% reduction in greenhouse gas emissions; (ii) 32% renewable energy in the final energy mix; and (iii) 32.5% energy efficiency improvement. The transport, building and industry sectors are currently the main sources of greenhouse gas emissions in the *EU* [4]. The development of renewable energy technologies to replace fossil fuels in electricity generation has been a focus of research for several decades now. Some of these studies analysed whether renewable energies are ready to support the current and future energy demand.

Solar energy has the potential to play a key role in reducing greenhouse gas emissions because it is abundant, safe, reliable and non-polluting. Solar technologies that can be used to generate electricity include photovoltaic (*PV*) and concentrated solar power (*CSP*). *PV* technology is a growing technology for electricity generation [5] and is the subject of this study. *PV* power plants have a flexible architecture that allows them to be adapted to different locations [5]. This technology is subject to intermittency and fluctuations in power generation. The intermittent nature of the solar resource refers to the fact that the amount of solar energy that can be captured and converted into electricity using *PV* systems varies depending on the time of day, season, and weather conditions [6]. These fluctuations in the availability of solar energy can make it challenging to integrate solar PV into the electricity grid and ensure a stable and reliable supply of electricity. To address this issue, several approaches have been developed, including energy storage systems, such as pumped hydroelectric storage power plants. This feature puts *PV* technology at a disadvantage compared to *CSP* technology, which allows energy storage. Therefore, overcoming the possible fluctuating operation of a *PV* plant due to random weather would put this type of technology in a privileged position. However, the joint operation of a *PV* power plant with a pumped hydroelectric storage power plant can also achieve energy storage. In other words, to achieve a reliable energy source, one can combine sources with strong temporal complementarity, such as photovoltaics, and couple them with some kind of energy storage device, such as a pumped hydroelectric storage power plant.

There are three main types of hydropower plants [7]: impoundment, diversion, and pumped storage. However, it is important to note that impoundment and diversion hydropower plants typically use dams to control the flow of water and create a head of water to drive turbines. Pumped storage hydropower plants also require two reservoirs, with one located at a higher elevation than the other, which can be created by building dams. However, there are also run-of-river hydropower plants that do not require a dam and instead use the natural flow of a river or stream to drive turbines. Tidal and wave energy converters are also considered types of hydropower facilities that do not require dams. In this study, we are interested in hydroelectric power plants with reservoirs, in particular, pumped hydroelectric storage power plant.

A pumped hydroelectric storage (*PHS*) power plant consists of an upper and a lower reservoir connected to a penstock, and a reversible pump turbine (See Figure 1). When electricity is to be generated (generation mode), water flows through the penstock to drive the hydro turbines. When the hydraulic machine operates as a pump (pumping mode), the water changes direction and is pumped from the lower tank to the upper tank. In pumping mode, energy from an external source (e.g., the grid or a *PV* plant) powers the pumps. Energy from solar production can be stored under this operating mode.

Some of the operating characteristics of these plants can be summarised as follows: (i) flexibility in start and stop operations, and (ii) a fast response speed so that it can adapt to drastic load changes and, therefore, follow load changes. These operating characteristics enable them to play a balancing role in electrical systems, providing reliability to the system. This advantage is enhanced by the increasing share of intermittent energy sources in the

electricity market, such as photovoltaic technologies. Therefore, the flexible characteristics of this type of plant are expected to be used more extensively. In addition to the advantages mentioned above, the integration of *FPV* and *PHS* systems has the following advantages for the *PHS* system:

(i) Water savings. Water savings are due to the reduction in water evaporation due to the partial coverage of the reservoirs in the *PHS* systems. This value is estimated to depend on climate conditions and the percentage of area covered [8].

(ii) Water quality. In terms of water quality, the lack of light produced by partial water cover creates algae blooms [9].

Over the last three years, the analysis of floating photovoltaic (*FPV*) systems has been an emerging topic in scientific literature [10]. 89% of the studies conducted on floating *PV* systems focused on reservoirs for hydroelectric generation [10–13]. Therefore, the study of the joint mode of operation of these power generation systems is an important line of research. Floating *PV* plants have *PV* modules and solar inverters similar to ground-mounted *PV* plants. However, the mounting system of the *PV* modules is very different. The different components in this type of plant are [8] a main floating body, a connection floating body, and a mooring system. The profits obtained by an *FPV* system due to its integration in a *PHS* system are as follows:

(i) No land occupancy. The large land area occupied by ground-mounted *PV* plants competes with agricultural or green zones [14]. With *FPV* plants, this disadvantage is resolved.

(ii) Cooling of the *PV* modules. *PV* modules profit from the cooling provided by water. This considerably increases the electrical efficiency of the *PV* modules, resulting in 2.33% [15] to 10% [16] more energy per year.

In the 1990*s*, the countries of the European Union liberalised their energy systems. The evolution from heavily regulated to liberalised electricity markets was similar in the different countries, as it took place within the framework of common European legislation. The concept of exchange-based zonal markets is the spirit of electricity markets [17]. The electricity supply structure, the price mechanism, the trading mechanism, and the market agents are regulated by the electricity market. The electricity market is responsible for maintaining the balance in the electricity system, as supply (generation) and demand (load) must be continuously balanced in real time to maintain the reliability of the system.

Therefore, there are two systems—*FPV* and *PHS*—which have to be adapted to the conditions of the electricity market. Several modes of operation are possible: (i) an independent operation mode, (ii) a joint operation mode, and (iii) an energy storage operation mode. With the first mode, the two plants operate independently by selling electricity. With the second mode, the two plants operate jointly selling electricity, but the energy generated by the *FPV* plant can be sold as it is generated or it can be used in the pumping process of the *PHS* plant so that the *PHS* plant can then sell electricity at the most appropriate times. Finally, with the third mode, the two plants operate jointly storing energy. Choosing the right mode of operation according to electricity market conditions poses a challenge for such systems. Figure 1 shows a diagram reflecting the interaction between the three systems studied.
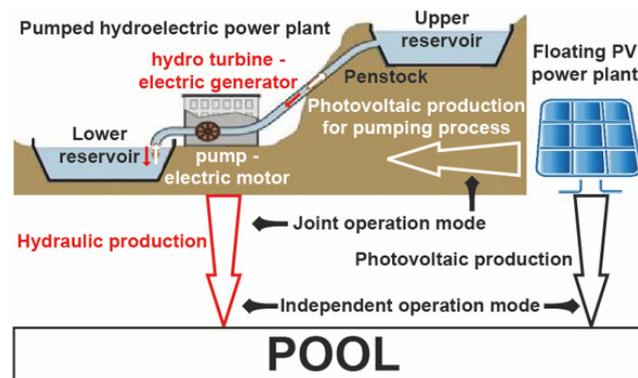
Figure 1. Representation of the three systems under study [18].

The feasibility and cost effectiveness of integrating *FPV* systems in *PHS* power plants have been extensively studied in the literature [19–22]. Although this type of configuration was initially used in the electrification of remote areas without access to the public grid, it has nowadays been extended to large *PHS* power plants.

Rauf et al. [23] evaluated the integration of a 200 (*MWp*) *FPV* power plant into an existing conventional 1450 (*MW*) hydropower plant in Pakistan. The results showed additional energy production of more than 3.5% when the conventional hydropower plant was combined with an *FPV* system. Kocaman and Modi [24] investigated the cost effectiveness of integrating *FPV* plants into *PHS* and conventional hydroelectric systems. The results showed that *PHS* systems allow a higher solar energy capacity to be installed in an affordable manner than conventional hydropower systems. Therefore, the integration of *FPV* systems into *PHS* systems is more cost effective than conventional hydropower systems. These two studies did not take into account electricity market conditions.

Glasnovic and Margeta [25] presented a hybrid system consisting of a *PHS* plant and an *FPV* plant to provide a continuous power supply. The energy supplied by the *FPV* power plant was used for the water pumping process of the *PHS* power plant. The energy produced by the *PHS* plant was used to supply electricity to isolated consumers. This paper only considered one of the possible modes of operation of the proposed system. In addition, the electricity market conditions are not taken into account.

Due to climate change, decreasing rainfall causes water shortages in some hydroelectric power plant reservoirs. As a result, some hydroelectric power plants remain out of service for a few months of the year. Bhattacharjee and Nayak [26] analysed the impact of an *FPV* power plant on restoring the constant annual output of a *PHS* power plant. The results corroborate that this hybrid system is a viable option for restoring the constant annual yield from a *PHS* power plant.

In addition to the references provided above, Jurasz et al. [19] presented a detailed literature review on the joint operation of *FPV* and *PHS* systems. These authors stated that there are a limited number of papers directly dedicated to the joint operation of an *FPV* and a *PHS* plant operating in a day-ahead market. The following are some of the few papers that address this issue. Jurasz et al. [19] presented an efficient trading strategy for *FPV* and *PHS* systems operating in a day-ahead market. The presented model takes into account several uncertainties, such as inflow and solar irradiance in a simplified approach. Study [18] presented analyses of different scenarios of joint operation of *FPV* and *PHS* plants as well as the optimal operating strategy for the day-ahead Iberian electricity market, depending on the accuracy of the forecasts.

Considering that the inclusion of electricity market conditions has been barely discussed in the scientific literature, the main objective of this paper is to analyse how certain parameters of the two electricity generation systems affect their mode of operation in the Iberian electricity market. For this purpose, we analyse two parameters of a system consisting of an existing *PHS* power plant and an *FPV* power plant to be integrated, taking into account the conditions of the Iberian electricity market. These parameters are the size

of the *FPV* power plant and the efficiency of the pumping process of the *PHS* power plant. The indicators used to evaluate the study are the water volume gain and the economic benefit. This study will be carried out at one of the hydroelectric reservoirs in Portugal, i.e., the Alto Rabagão hydroelectric power plant, to assess the influence of the three parameters on the feasibility of installing a large-scale *PV* system.

The main contributions of this work are as follows:

(i)   Analysing the size of a floating *PV* power plant under Iberian electricity market conditions. To do so, the available reservoir area, terrain elevations, and existing electrical infrastructure at the pumped-storage hydroelectric power plant must be estimated.

(ii)   Analysing how the efficiency of the pumping process of the hydroelectric power plant affects the mode of operation of both plants under Iberian electricity market conditions.

(iii)   Analysing the energy storage possibilities of a floating *PV* power plant when both plants are operated under Iberian electricity market conditions.

(iv)   Analysing the optimal mode of operation of an integrated floating *PV*-hydroelectric power plant in order to obtain the maximum economic benefit.

In summary, the purpose of this work is to facilitate decision making in the mode of operation of both power plants under electricity market conditions. The case studies make it possible to determinate the optimal answer to the following practical questions: What size does the *FPV* power plant have to be in order for both plants to be better adapted to the electricity market? What is the appropriate mode of operation of both plants? What is the economic benefit from changing the turbine-pump of the *PHS* power plant? Finally, how does the installation of an *FPV* power plant affect the water volume of the upper reservoir of a *PHS* plant? Establishing the answers to these questions would facilitate the design of *FPV* power plants and the joint operation of both plants.

This paper is structured as follows: Section 2 provides the context for the case study location. Section 3 describes the methodological approach to the operation of a floating PV power plant integrated with a pumped hydro power plant in the day-ahead market. The results are presented in Section 4. Finally, Section 5 summarises the main contributions and conclusions of the paper.

2. Context for the Case Study Location

The Iberian Peninsula, comprising Spain and Portugal, is a typical case of an area of high solar potential and growing energy demand. Renewable energies have been widely accepted by the population of the Iberian Peninsula; there were 15.4 (*GWp*) installed photovoltaic systems in operation at the end of 2021 [4]. The installed capacity of hydroelectric power plants was around 23.5 (*GW*) at the end of 2021 [4].

Most electricity is sold in *EU* member states through day-ahead markets [27]. In these markets, the hourly price of electricity depends on supply (amount and sources of energy available) and demand.

Portugal and Spain operate the same electricity market (Iberian Electricity Market, *MIBEL* by its acronym in Spanish). This market was created in 2004. *MIBEL* includes two main markets, where most transactions are carried out: the day-ahead market and the intra-day market. However, energy is mainly traded on the day-ahead market. In addition, it has the technical restrictions market and the complementary services market, where the number of transactions is lower. In this type of market, there are two main agents called the market operator and the system operator. The market operator is the market manager of the day-ahead and intra-day market. In *MIBEL*, it is called *OMIE*, for its Spanish acronym. The system operator is the market manager of the technical restrictions market and complementary services market. The system operator in Portugal is called *REN*, and in Spain, it is called *REE*.

OMIE uses the marginalist model for its transactions. In this model, electricity producers make their bids based on the marginal cost of production. This model includes

all costs, such as the cost of emissions, the cost of fuel, the variable cost of operation and maintenance. It also includes taxes.

2.1. Description of the Day-Ahead Market

The operating principle of the day-ahead market is that of an auction. As in any auction, there are two types of agents: selling agents and buying agents. The generating plants and energy importers are the selling agents. The traders who resell their energy on the retail market or export it and the end consumers who use the wholesale market are the buying agents.

The mechanism of operation of the day-ahead market is as follows: (i) On day $D - 1$, at 12:00, selling agents submit the electricity bid for each hour of day D. (ii) On day $D - 1$, at 12:00, buying agents submit the purchase offer for each hour of day D. (iii) On day $D - 1$, $OMIE$ builds the supply and demand curves according to the criteria shown in Figure 2.

The intersection of the supply and demand curves determines the market price for each hour of day D. Therefore, all matched sell (buy) bids are charged (paid) at the same price. Figure 2 shows an example of this procedure.
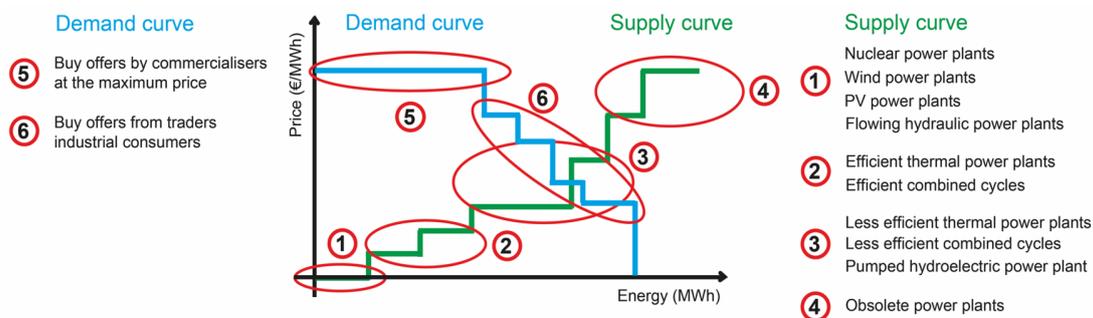
Figure 2. Supply and demand curve.

The supply and/or demand for each hour of day D may vary, resulting in an imbalance. Several reasons can cause such an imbalance: (i) generation failures, (ii) transmission failures, and (iii) variations in expected weather conditions. An imbalance in the system is called a deviation. Therefore, the deviation is the difference between the predicted power and the actual power available. Deviations can be classified according to their direction: upward deviation and downward deviations.

From a power plant perspective, there is an upward deviation when there is overproduction and a downward deviation when there is underproduction. By contrast, on the demand side, there is an upward deviation when there is a shortfall in consumption, and a downward deviation when there is overconsumption. When a deviation occurs, a payment obligation may occur, depending on the market's needs.

Market needs in the Iberian Electricity System are determined by the concept known as the net system balancing need ($NNBS$, by its acronym in Spanish). This indicator examines whether the total production is higher or lower than the scheduled production. Therefore, the $NNBS$ determines whether the production deviation is favourable or detrimental to the electricity system. Two situations can occur:

(i) If $NNBS > 0$, the net production of the electricity system is lower than scheduled in the market and thus more energy is required.

(ii) If $NNBS < 0$, the net production of the electricity system is greater than scheduled in the market and thus less energy is required.

According to the $NNBS$ indicator, deviations can be classified according to whether they are in favour or against the market:

(i) Deviation in favour. This is a deviation that occurs in the same direction as the market need. For example, the power plant produces less energy than scheduled and the

$NNBS < 0$, or when the power plant produces more energy than scheduled and the $NNBS > 0$.

(ii) Against deviation. This is a deviation that occurs in the opposite direction to the market need. For example, the power plant produces less energy than scheduled and the $NNBS > 0$, or when the power plant produces more energy than scheduled and the $NNBS < 0$.

Deviations have an economic impact, which are either positive or negative. Therefore, deviations in favour are associated with a price (PUD/PDD) and deviations against are associated with a cost (CUD/CDD). $OMIE$ sets the PUD and the PDD. The cost of deviation CUD (CDD) is the difference between the absolute value of the marginal market price and the PUD (PDD).

2.2. Case under Study

The Alto Rabagão pumped hydroelectric storage power plant is located in the district of Vila Real in Northern Portugal (latitude $41°44'16''$ N, longitude $7°51'14''$ W, and altitude of 880 (m)) [28]. The project is led by the Portuguese energy company EDP. The upper reservoir of the Alto Rabagão has already been built. The surface area is 2200 (ha), and it has a volume of 569 (hm^3), and a maximum water level of 185 (m) [28]. The River Rabagão feeds this reservoir. In order to guarantee the environmental flow of the lower part of the river, the power plant always discharges a part of the flow without generating electricity. In this case, the reserved volume is 11 (hm^3). Figure 3 shows a Google Earth image of the Alto Rabagão pumped hydroelectric storage power plant.
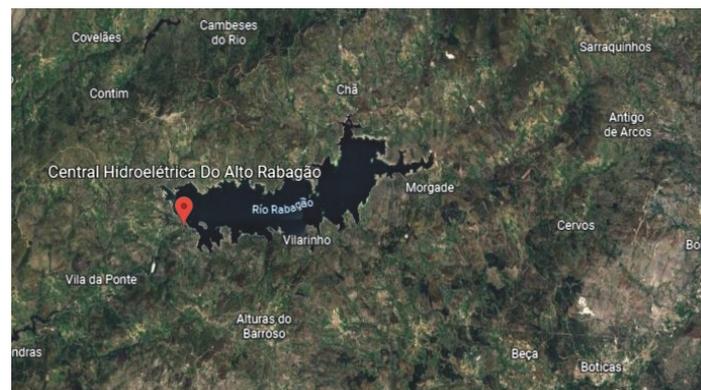
Figure 3. Google Earth map of the Alto Rabagão PHS power plant.

This hydroelectric power plant was commissioned with a total output of 67 (MW) in the year 1964 [28]. This plant uses 2 binary groups (hydro turbine-pump) [28]. The total power in pumping mode is 62 (MW) [28]. Obviously, the total maximum flow rate is not the same in generation mode as in pumping mode. These values are 46.5 (m^3/s) and 33 (m^3/s), respectively [28].

3. Methodology

When the objective of the FPV–PHS system is to maximise economic benefits by offering energy in the day-ahead market, the aim is to sell the available energy during the times when market prices are the highest. Under these conditions, the uncertainty provided by the FPV system is a major drawback. Therefore, analysing the size of the FPV plant can help make the right decision.

In order to achieve the objectives sought with this study, the following methodology is proposed:

(i) Deducing possible modes of operation.
(ii) Parametric analysis.
(iii) Meteorological data selection.

(iv) *FPV* power plant design.

(v) *FPV* power plant size

The first step is to define the possible modes of operation of both plants under the Iberian electricity market conditions. In the second step, the parameters of the power plants that make up the system will be identified and those that may influence the mode of operation of both power plants under electricity market conditions will be analysed. The third step is the selection of meteorological data. The step before calculating the photovoltaic energy is to select the meteorological data from the location of the pumped-storage hydroelectric power plant. Obtaining the energy generated by the floating *PV* plant per square metre of *PV* field is the fourth step of this methodology. Finally, step 5 defines the indicator used to evaluate the operating model for both plants.

3.1. Deducing Possible Modes of Operation

The size of a floating *PV* plant determines the mode of operation of both plants in the electricity market. In addition, the efficiency of the pumping process is also a factor conditioning the mode of operation of both power plants. Therefore, the possible modes of operation of both plants under electricity market conditions must be determined.

The possible modes of operation, regardless of market conditions, are as follows:

(i) Continuous operation of the hydropower plant, i.e., 24 h a day, is a mode of operation that would deplete the available water in the upper reservoir, meaning there would not be a sufficient annual flow to maintain the required average flow at full power. Therefore, the mode of operation of a hydroelectric power plant is intermittent. Forecasting the times with the highest energy prices determines the operating times of the hydropower plants. The water stored in the upper reservoir is conserved for use during the times that provide the greatest economic benefit. The rest of the time, it can operate in pumping mode. Due to the mode of operation of these plants, the transmission lines to the grid also operate intermittently. Therefore, they can be used by a floating *PV* plant.

(ii) Selling electricity as it is generated would be the operation mode of a floating *PV* power plant without the possibility of storing energy (Mode *A*). If the floating *PV* power plant has a storage system, as in this case, another mode of operation is to store electricity, in the form of stored water, as it is generated (Mode *B*). To do this, water would be pumped from the lower reservoir to the upper reservoir. In this way, a greater economic benefit could be obtained by turbining this water at times of high prices. Considering Modes *A* and *B*, it is also possible to sell and store electricity simultaneously as it is generated (Mode *C*).

The decision to use one mode of operation or another is determined by the electricity market conditions. Five cases are possible:

(i) Case 1: No deviation. This would be the ideal case (a highly unlikely situation). The energy bid on day $D - 1$ coincides with the energy available on day D. This case is characterised by the absence of a penalty, as there are no deviations. The marginal market price would be the selling price. The floating *PV* plant operates in Mode *A* (selling electricity as it is generated). The two power plants operate independently.

(ii) Case 2: An upward deviation (energy bid on day $D - 1$ is less than the energy available on day D) and $NNBS > 0$. As the deviation is in favour of the system, there is no penalty, and a collection right is generated. The marginal market price would be the selling price. The floating *PV* plant operates in Mode *A* (selling electricity as it is generated). The two plants operate independently of each other.

(iii) Case 3: An upward deviation (energy bid on day $D - 1$ is less than the energy available on day D) and $NNBS < 0$. As the deviation goes against the system, the right to be charged for the surplus energy will be lower than the marginal market price. Therefore, the floating *PV* plant may store the surplus energy in order to sell it on another day at the marginal market price. The floating *PV* plant operates in Mode *C*. The joint

operation of the two plants may be the best option. In this case, the size of the floating *PV* plant will be a determining factor in the choice of its mode of operation. The efficiency of the pumping process also influences the choice.

(iv) Case 4: An downward deviation (the energy bid on day $D - 1$ is greater than the energy available on day D) and $NNBS > 0$. As the deviation is against the system, a payment obligation is generated. This price is higher than the market price. Therefore, it is the worst situation for the floating *PV* plant as the plant loses money. The floating *PV* plant operates in Mode *A* (selling electricity as it is generated). The mode of operation will be joint, as the pumped hydroelectric power plant helps to cover the energy imbalance of the floating *PV* power plant.

(v) Case 5: An downward deviation (the energy bid on day $D - 1$ is greater than the energy available on day D) and $NNBS < 0$. As the deviation is in favour of the system, there is no penalty. The marginal market price would be the selling price. The floating *PV* plant operates in Mode *A* (selling electricity as it is generated). The two plants operate independently of each other.

3.2. Parametric Analysis of a Pumped Hydroelectric Storage Power Plant

A pumped hydroelectric storage power plant has a configuration of two water reservoirs (upper and lower reservoirs) at different heights, connected by penstocks. In generation mode, power is generated as water flows down the penstock from one reservoir to the other, passing through a turbine that is coupled to an electric generator. Once the water has been turbined, it is stored in the lower reservoir. Therefore, this system acts similarly to a battery, as it can store energy and release it when needed. In pumping mode, the system absorbs electrical energy as it pumps water back to the upper reservoir. In this mode of operation, the electric generator functions as a motor and the hydraulic turbine as a pump. This system generally uses a single penstock, which is used in both modes of operation.

The power flow is bidirectional depending on the operation mode. Therefore, each mode of operation, generation mode and pumping mode, will have certain parameters.

3.2.1. Generation Mode

The parameters involved in the generation mode are the available head (h_a), the turbined flow rate (q_t), the density of water (ρ), the acceleration due to gravity (g), the electric generator efficiency (η_g), and the hydro turbine efficiency (η_t). Therefore, the hydroelectric power can be calculated using Equation (1) [26]:

$$P_g = P_t \cdot \eta_g = \eta_t \cdot \rho \cdot g \cdot h_a \cdot q_t \cdot \eta_g \tag{1}$$

As the hydroelectric power plant is built, the parameter h_a can be considered to remain constant, as replacing the penstocks or modifying h_a would not be a cost that can be assumed. The replacement of the turbine and the electric generator, although costly, could be feasible.

Another aspect to be taken into account is the variation of the water level in the upper reservoir. When the upper reservoir has a large capacity, several studies have considered this parameter to be constant over the operation interval [26,29].

3.2.2. Pumping Mode

The parameters involved in the pumping mode are the elevating head (h_e), the pumped flow rate (q_p), the density of water (ρ), the acceleration due to gravity (g), the electric motor efficiency (η_m), and the pump efficiency (η_p). Therefore, the electrical power absorbed in the pumping process can be calculated using Equation (2) [26]:

$$P_a = \frac{\rho \cdot g \cdot h_e \cdot q_p}{\eta_m \cdot \eta_p} \tag{2}$$

Following the same reasoning as above, it can be considered that the parameter h_e remains constant, and that the substitution of the pump and the electric motor is admissible.

Next, the two modes of operation are related. For this purpose, the following parameters are defined: the turbine generating coefficient (k_t), the water pumping coefficient of the pumping process (k_p), and the total process efficiency (μ). The following are the equations:

$$k_t = \eta_g \cdot \eta_t \cdot \rho \cdot g \cdot h_a \tag{3}$$

$$k_p = \frac{\rho \cdot g \cdot h_e}{\eta_m \cdot \eta_p} \tag{4}$$

$$\mu = \frac{k_t}{k_p} = \eta_g \cdot \eta_t \cdot \eta_m \cdot \eta_p \tag{5}$$

For water pumped and then used for generation, all efficiency factors are applied in both pumping and production modes. The following is therefore fulfilled:

$$P_g = k_t \cdot q_t \tag{6}$$

$$P_a = k_p \cdot q_p = \frac{k_t}{\mu} \cdot q_p \tag{7}$$

The typical μ of this type of hydroelectric plant ranges from 65% to 80%, depending on the technical characteristics of the equipment [30]. Obviously, the lower value corresponds to older plants. Other studies estimate that a maximum of 70% to 85% of the electrical energy absorbed from the grid can be recovered for the pumping process [29]. Technological advances over the last 25 years have resulted in modern systems with μ of up to 87% [21].

The Alto Rabagão pumped-storage hydropower plant has a turbine generation coefficient (k_t) of 1.44086 (MWs/m^3), and the total efficiency of the pumping process (μ) is 0.77 [28].

Taking into account the volume of water available, the Alto Rabagão pumped-storage hydroelectric power station operates at full power for 4 h a day [28]. Therefore, the energy generated each day is 268 (MWh).

There are several parameters that can be used to evaluate and analyse *PHS* power plants, such as (i) capacity, (ii) total process efficiency, (iii) energy yield, (iv) power output, (v) cost, (vi) environmental impact, (vii) cycle time, (viii) maintenance requirements, and (ix) lifetime. As the PHS plant is already built and the impact of the implementation of an FPV plant in its upper reservoir is analysed, parameter (ii) is considered to be appropriate. The influence of the parameter μ on the joint operation of both plants is analysed in this paper. The parameter μ is 0.77 in old plants. In contrast, this parameter is usually 0.85 in modern plants.

3.3. Parametric Analysis of a Floating PV Power Plant

The main component of a floating *PV* plant is the *PV* modules; therefore, the parameters of this type of plant are related to this element. These parameters are the technology used to manufacture of the *PV* module (solar transmittance of glazing (τ), and solar absorptance of *PV* layer (α)), the number of *PV* modules (N_{PV}), the module dimensions (module width (W_{PV}), module length (L_{PV}) and module surface (A_{PV})), the efficiency electrical of the *PV* module (η_e), the available solar resource, the tilt angle of the *PV* module (β), and the orientation of the *PV* module (γ). The last three parameters are included in the incident solar irradiance parameter (I_t). Therefore, the power generated by a floating *PV* power plant can be calculated using Equation (8) [31]:

$$P_{PV} = N_{PV} \cdot A_{PV} \cdot (\tau \cdot \alpha) \cdot I_t \cdot \eta_e \tag{8}$$

3.3.1. Technology Used to Manufacture of the *PV* Module

Currently, there are three *PV* module technologies: monocrystalline, polycrystalline and thin film (*CdTe*). These three technologies have different electrical efficiencies. However, in this section, we are interested in the transmittance–absorption product. The commonly used value of the transmittance–absorption product ($\tau \cdot \alpha$) is 0.9 [32,33].

3.3.2. Electrical Efficiency

Electrical efficiency is defined as the efficiency of the module to convert incident solar irradiance into electrical energy. This efficiency depends on the type of manufacturing technology used for the *PV* module. The manufacturer of the *PV* module provides the electrical efficiency (η_{ref}) at the reference temperature (T_{ref}) of 25 (°C) and a solar irradiance of 1000 (W/m^2). To obtain the electrical efficiency (η_e) under other conditions of temperature (T_c) and solar irradiance (I_t), the equation provided by Evans [34] is often used [35,36]. This equation is as follows [34]:

$$\eta_e = \eta_{ref} \cdot \left[1 - \beta_{ref} \cdot \left(T_c - T_{ref} \right) \right] \tag{9}$$

where β_{ref} is the temperature coefficient; (1/^{o}C) is normally provided by the *PV* module manufacturer.

According to the literature, if the operating temperature of the *PV* modules exceeds 25 (°C), the electrical efficiency decreases [36,37]. The effects of the ambient temperature, the incident solar irradiance and the wind speed must be considered. The number of models for predicting the operating temperature of a *PV* module is high [38]. Dutra et al. [37] show 20 models in their work. One such model is presented by Mattei et al. [39], which offers satisfactory results. This model uses the normal operating cell temperature (*NOCT*). This parameter is provided by the *PV* module manufacturer. This model uses the ambient temperature (T_a), the solar irradiance (I_t) and the *NOCT* (determined under the following conditions: 800 (W/m^2) of solar irradiance, 20 (°C) of ambient temperature and 1 (m/s) of wind speed at the height of the *PV* module). The proposed equation is as follows:

$$T_c = T_a + (NOCT - 20) \cdot \frac{I_t}{800} \tag{10}$$

The electrical efficiency of *FPV* plants is higher than that of ground-mounted *PV* plants. This increase depends on the environmental conditions at the installation site: (i) For Choi [40], efficiency increases up to 11%. (ii) For Liu et al. [16], the efficiency increases up to 10%. (iii) For Oliveira-Pinto and Stokkermans [41], the efficiency ranges from 0.31% to 2.59%. (iv) For El Hammoumi et al. [15], the efficiency increases up to 2.33%.

3.3.3. Incident Solar Irradiance

The equation proposed by Duffie and Beckman [42] is usually used to determine the total solar irradiance $I_t(n, T, \beta)$ on tilted surfaces:

$$I_t(n, T, \beta) = I_{bh}(n, T) \cdot \frac{\cos \theta_i}{\cos \theta_z} + I_{dh}(n, T) \cdot \left(\frac{1 + \cos \beta}{2} \right) +$$
$$+ (I_{bh}(n, T) + I_{dh}(n, T)) \cdot \rho_g \cdot \left(\frac{1 - \cos \beta}{2} \right) \tag{11}$$

where I_{bh} is the beam irradiance on the horizontal plane, I_{dh} is the diffuse irradiance on the horizontal plane, θ_z is the zenith angle of the sun, θ_i is the incident angle calculated using the equation proposed by Duffie and Beckman [42], β is the tilt angle, and ρ_g is the ground reflectance.

According to the above, the energy supply must be hourly. For this purpose, Equation (11) is integrated from sunrise (T_R) to sunset (T_S) in one-hour intervals:

$$H_t(n, \beta) = \int_{T_R(n)}^{T_S(n)} I_t(n, T, \beta) dT \tag{12}$$

where H_t is the total solar irradiation, n is the day of the year, and T is the solar time.

3.3.4. Number and Dimensions of *PV* Modules

Once the location of the *PHS* power plant, the tilt angle, the orientation, the *PV* module technology, and the model of the *PV* module used have been defined, the only parameter that will influence the size of the floating *PV* power plant is N_{PV}. This value is determined in the section on the optimisation of the floating *PV* power plant.

There are several parameters that can be used to evaluate and analyse *FPV* power plants: (i) capacity, (ii) efficiency, (iii) energy yield, (iv) cost, (v) environmental impact, (vi) maintenance requirements, and (vii) durability. Although all parameters are important, parameters (i), (ii) and (iii) are adapted to the subject matter of this work, as the size of the *FPV* power plant encompasses these parameters.

3.4. Meteorological Data Selection

The third step is the selection of meteorological data. The previous step in the calculation of the photovoltaic energy is to select the meteorological data from the location of the *PHS* power plant.

Precise knowledge of the amount of incident solar irradiance on a horizontal surface is essential to optimising the *FPV* plant. However, it is unlikely that a weather station is available at the dam to record global and diffuse solar irradiance over the horizontal surface. For this reason, using a proven solar model, such as the one proposed in [43], is necessary. This model has been validated with real data from weather stations [44], and has been used in similar studies, as it more accurately predicts solar irradiance under different climate conditions [18,45,46]. In addition, meteorological data must be expressed in hours, as this is the time interval used in the Iberian electricity market. The method presented by [43] meets these specifications, as it determines the hourly beam and diffuse solar irradiance on a horizontal surface under the meteorological conditions of a specific location and for each day of the year. This method follows three steps: (i) Hottel's clear-day model [47] to estimate the solar irradiance transmitted through a clear atmosphere; (ii) Liu and Jordan's clear-day model [48] to determine the diffuse solar irradiance for clear skies; and (iii) Fourier series approximation to adapt the clear-sky models to the meteorological conditions of the reservoir. Therefore, the I_{bh} and I_{dh} values of Equation (11) are determined by the method proposed in [43].

Monthly beam and diffuse solar irradiation on horizontal surfaces are necessary to apply the method [43]. The data should cover at least 10 years of meteorological measurements to build a good picture of the local climate, thus reducing the uncertainty that could be caused by using meteorological data from a specific year. Although there are several sources of meteorological data available, this method uses the *PVGIS* tool [49], an *EU* project which provides freely accessible solar radiation databases. Specifically, the *PVGIS-SARAH*2 database, with data which are satellite based and a time period from 2011 to 2020, was used.

Figure 4 shows the monthly beam and diffuse solar irradiation on horizontal surfaces at the Alto Rabagão dam obtained using the *PVGIS* tool [49]. Figure 5 shows the results obtained using the method proposed in [43] for beam and diffuse solar irradiation on a horizontal surface under the meteorological conditions at the Alto Rabagão dam.

The monthly mean daytime and nighttime temperatures are presented in Figure 4. The average monthly maximum daytime temperature is 27.7 (°C), and the average monthly maximum night-time temperature is 14.9 (°C).
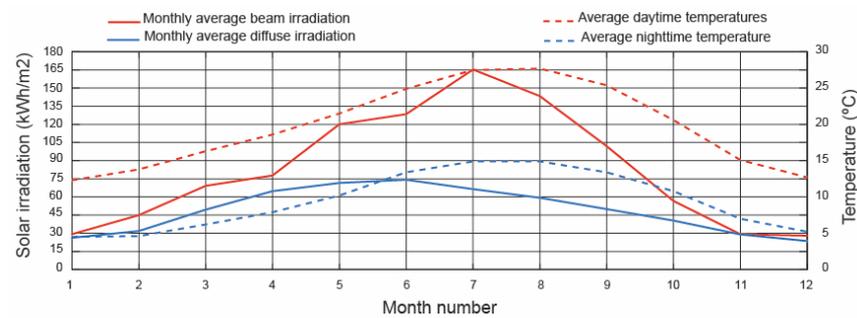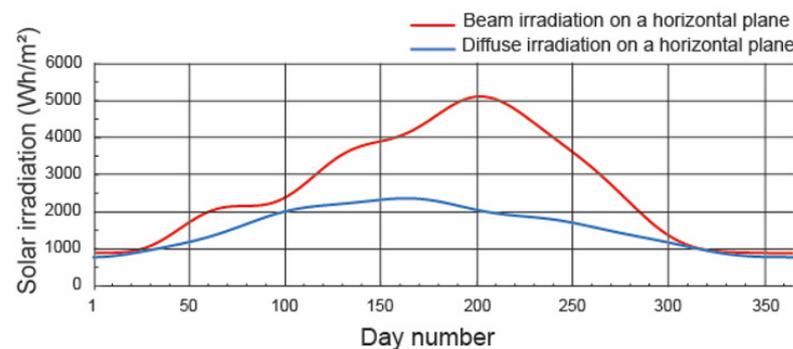
Figure 4. Environmental conditions.

Figure 5. Beam and diffuse solar irradiation on a horizontal surface.

3.5. The FPV Power Plant Design

The design of a ground-mounted photovoltaic plant has been studied by several authors [31,46]. In contrast, there are few studies on *FPV* power plants from this point of view [50].

The following considerations have been taken into account in this study:

(i) The shape of the available area. In ground-mounted *PV* power plants, the irregular shape of the ground greatly influences the design [46]. In the case of *FPV* power plants, complex irregular shapes are not possible due to the nature of the floating platform. Therefore, the design of *FPV* power plants is more similar to designs with regular shapes [51]. The dimensions of the main floating body component chosen defines the shape of the *FPV* power plant. The system chosen for mounting the *PV* modules uses two main floating bodies. Each of them has the following dimensions: $1160 \times 935 \times 370$ (mm) [52]. The usual shape of *FPV* power plants is rectangular, or they can be decomposed into this type of shape [53,54].

(ii) The tilt angle. Another aspect is the tilt angle of the *PV* modules. In ground-mounted photovoltaic plants, the tilt angle is chosen to maximise the incident solar irradiance on the *PV* modules. This tilt angle is related to the latitude at the site. In *FPV* power plants, on the other hand, the tilt angle is chosen to ensure the stability of the *PV* modules. Therefore, tilt angles are chosen that are not related to the latitude at the site. With *FPV* systems, the tilt angle is chosen in accordance with the stability of the floating platform. The tilt angle of a *PV* module must avoid the detrimental effects of wind loads, waves and water currents. Therefore, floating platforms limit the tilt angle of *PV* modules. Specifically, there are three standard values for tilt angles: 5 (°) [52,55], 12 (°) [56]. In [18], the *FPV* power plants using each of these tilt angles are summarised.

Floating platforms with a tilt angle of 5 (°) [52,55] are chosen. They can withstand wind loads of 180 (km/h).

(iii) The orientation. As is the case with ground-mounted photovoltaic plants, the use of an optimal orientation is not a problem. Therefore, the optimum orientation is 0 (°) in

the northern hemisphere and 180 (°) in the southern hemisphere [42]. As the chosen *PHS* power plant is in the northern hemisphere, an orientation of 0 (°) will be used.

(iv) The shading effect between modules. Due to the connecting floating body component, which connects the main floating bodies to each other, and the low tilt angle of the modules, the shading between *PV* modules will be quite low. However, the algorithm will take this into account.

(v) The albedo. Typical albedo values for different ground surfaces were calculated by [57–59]. Where no information is available, a value of 0.2 is often used [60]. In contrast, the albedo of water bodies ranges between 0.05 [16,41,50] and 0.07 [16]. Therefore, an albedo of 0.05 was used.

(vi) Only one commercial *PV* module model will be used. The model chosen is the JAM72S30 525-550/MR, which is manufactured by JASolar. The characteristics of the module are as follows: power, 550 (Wp); dimensions, 2279×1134 (mm); and surface area, 2.58 (m^2). The algorithm works for any *PV* module.

(vii) *FPV* power plant configuration. In ground-mounted photovoltaic plants, several rack configurations can be used [46]: $1V \times N_{PV}$, $2V \times N_{PV}$, $3V \times N_{PV}$, $2H \times N_{PV}$, $3H \times N_{PV}$, etc. In *FPV* systems, by contrast, the $1H \times N_{PV}$ configuration is typically used to minimise wind loads on the *PV* modules.

(viii) The transversal and longitudinal installation distance. The system chosen for mounting the *PV* modules uses two main floating bodies [52]. Each of them has the following dimensions: $1160 \times 935 \times 370$ (mm) [52]. The transverse maintenance distance is $e_t = 25$ (mm), and the longitudinal maintenance distance is $e_l = 378$ (mm) [52].

(ix) The number of *PV* modules. According to the dimensions of the *PV* modules and the main floating bodies, the basic configuration will be 10×20 *PV* modules. An almost square shape measuring 23.62×31.09 (m) ($A_T = 734.19$ (m^2)), and a power of 0.11 (MWp) is obtained with these configurations. This basic unit is surrounded by floating connecting bodies. The connection floating body acts as a foothold during the construction and maintenance of the *FPV* system. The dimensions of the connection floating bodies vary depending on the manufacturer. In this study, they have the following dimensions: $1097 \times 575 \times 240$ (mm) [52].

The algorithm used to determine the total energy is based on 3 steps: (i) the determination of total solar irradiance; (ii) the determination of the total surface area of the *PV* modules; and (iii) the determination of the total energy. These steps are explained in more detail below:

(i) The determination of total solar irradiance (H_t). This can be calculated using Equation (12) and the restrictions indicated above.

(ii) The determination of the total surface area of the *PV* modules (A_T). The total surface area of the *PV* modules (A_T) can be found with

$$A_T = \sum_{i=1}^{N_{PV}} W_{PV} \cdot L_{PV} \tag{13}$$

where N_{PV} is the number of *PV* modules, W_{PV} is the module width, and L_{PV} is the module length. The shadows that each row casts on the adjacent row in the longitudinal direction is an aspect taken into account by the algorithm designed.

(iii) The determination of the total energy. The total energy can be determined by the following equation:

$$E_{PV} = H_t \cdot A_T \tag{14}$$

3.6. The FPV Power Plant Size

The size of the *FPV* power plant can be chosen according to several criteria:

(i) The power of the *PHS* power plant. The power of the *PHS* power plant is 67 (MW) and its capacity is 973 (GWh).

(ii) The area available for deployment of *FPV* plant. The available area is 2200 (ha).

(iii) The volume of water in the upper reservoir. The size of the *FPV* power plant to supply the electrical energy required to raise the water level of the upper reservoir by a certain level by means of the pumping mode of operation of the *PHS* plant.

(iv) The pumping mode. The size of the *FPV* plant to supply the electrical energy required for the pumping mode of operation of the *PHS* plant.

(v) The number of operating hours of the *PHS* plant. The size of the *FPV* power plant to supply the electrical energy necessary to increase the number of operating hours of the *PHS* plant.

Each of these criteria is discussed in the Results section.

4. Results and Discussion

In this paper, the year 2022 was selected to frame the study presented. The daily hourly marginal market price (*MMP*), the price of upward deviations (*PUD*) and the price of downward deviations (*PDD*) can be found in [61]. Figure 6 shows the daily hourly marginal Iberian market price for the year 2022.
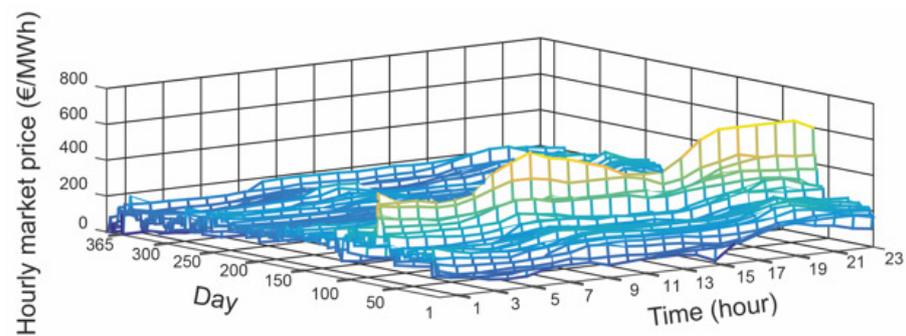
Figure 6. Daily hourly marginal Iberian market price for the year 2022.

Figure 7 shows the annual average hourly marginal Iberian market price for the year 2022. As can be seen in Figures 6 and 7, the four hours with the highest prices are 19:00, 20:00, 21:00 and 22:00. Therefore, these will be the hours of the *PHS* plant operation. The *FPV* plant will obviously not generate power during these hours.
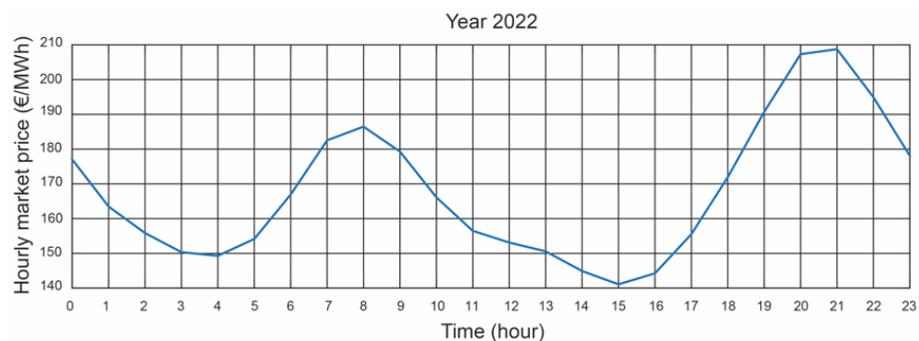

Figure 7. Annual average hourly marginal Iberian market price for the year 2022.

As the power of the *PHS* power plant is 67 (*MW*), the following power ratings for the *FPV* power plant are chosen as a starting point for the study: 33.55 (*MWp*) (50% *PHS*), 67.1 (*MWp*) (100% *PHS*), 100.65 (*MWp*) (150% *PHS*), 201.30 (*MWp*) (300% *PHS*), and 301.95 (*MWp*) (450% *PHS*).

Table 1 summarises the parameters of the *FPV* plant sizes studied based on the proposed methodology.

Table 1. Parameters of the FPV plant sizes studied.

Parameter	Size				
Designation	S1	S2	S3	S4	S5
Power (MWp)	33.50	67.10	100.65	201.30	301.95
Occupied area (hm^2)	22.39	44.78	67.18	134.35	201.53
Occupied area (%)	1.018	2.04	3.05	6.12	9.16
Number of total PV modules	61,000	122,000	183,000	366,000	549,000
Annual energy (GWh)	49.82	99.65	149.47	298.94	448.41

The capacity of all the plant sizes studied does not exceed the plant capacity of 973 (GWh).

Two values for the parameter μ are analysed in this paper. They are 0.77 for old *PHS* plants and 0.85 for modern *PHS* plants.

4.1. The Area Available for Deployment of an FPV Plant

In this case, an area of 2200 (ha) is available. According to Table 1, the surface area is not a limiting factor. The size of the plant could be further increased in accordance with the available area, but other aspects limiting the size of the *FPV* plant have to be analysed.
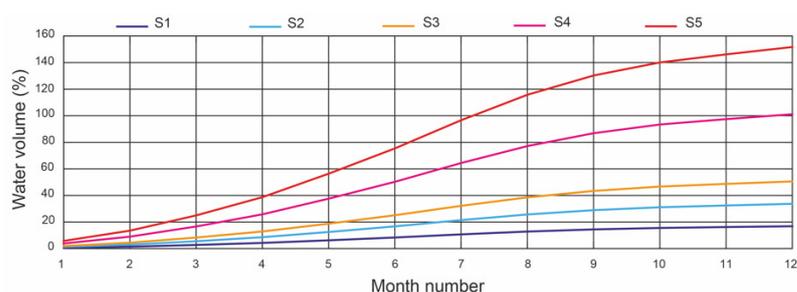
4.2. The Volume of Water in the Upper Reservoir

Water scarcity has become a topical issue. Water resources are necessary for human consumption and agriculture. The shortage of rainfall means that the upper reservoirs of the *PHS* power plants are not at their maximum capacity. For example, Figure 8 shows the water volume of the upper reservoir of the Alto Rabagão during the year 2022 [62]. The year 2022 was particularly dry. As a result, the upper reservoir level was approximately 20% for almost all the months of the year. The increase in volume in the last few months of the year is due to the *PHS* power plant operating in pumping mode, with the resulting loss in economic benefit.
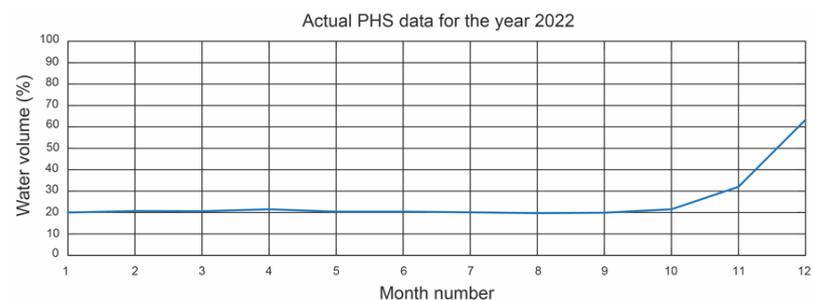
Figure 8. Volume of water in the upper reservoir in 2022.

Figure 9 shows the estimated water volume of the upper reservoir of the Alto Rabagão for different sizes of *FPV* plants if all the energy generated were to be used to pump water.

Figure 9. Volume of water in the upper reservoir.

The sizes of the analysed *FPV* plants occupy a very small water body compared to the total surface of the upper reservoir and reach remarkable upper reservoir levels. For example, size *S*1 occupies 1.018% of the upper reservoir and manages to pump a volume of water representing 16.85% of the upper reservoir. For size *S*2, these values would be 2.04% and 33.71%, respectively. For size *S*3, these values would be 3.05% and 50.56%, respectively. For size *S*4, these values would be 6.12% and 101.13%, respectively. For size *S*5, these values would be 9.16% and 151.69%, respectively.

As can be seen in Figure 9, the *S*5 size of the *FPV* plant obtains a water volume of more than 100%, so this power is not suitable. Similarly, larger sized *FPV* plants are not suitable.

The *S*4 sized *FPV* plant achieves 100% of the capacity of the upper reservoir. This is the limiting size for an *FPV* plant. All other sizes of *FPV* plants studied are suitable.

Therefore, sufficient energy can be stored for load management in the electricity grid with the *FPV* plant sizes studied (*S*1, *S*2, *S*3 and *S*4).

4.3. Usual Operation of the PHS Plant

The number of daily *PHS* plant operating hours is four. These four hours of operation correspond to the highest prices on the electricity market. In addition, the *PHS* plant operates under the conditions of Case 1: No deviation.

Figure 10 shows the daily energy generated with 4 daily hours of *PHS* plant operation during the year 2022. According to Figure 10, the number of *PHS* plant operating days is 71 days (20% of the days). The purpose of installing an *FPV* plant in the upper reservoir is for the *PHS* plant to operate 365 days a year.

The annual energy generated was 18.60 (GWh). This falls far short of its capacity, which is 973 (GWh). From an economic point of view, this earned EUR 4956259.88 from the sale of the energy generated.
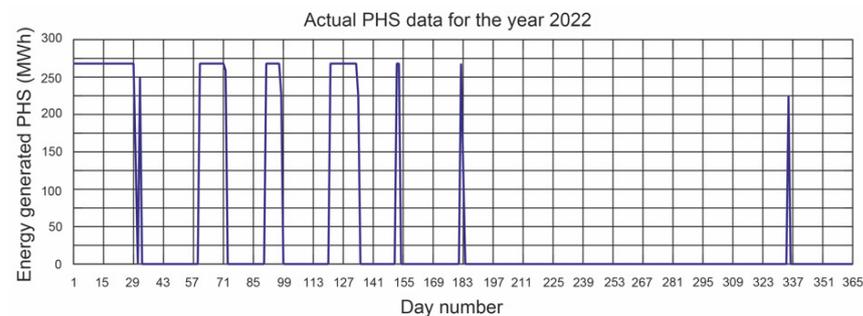

Figure 10. Daily energy generated by the PHS plant during the year 2022.

Figure 11 shows the daily energy absorbed during the pumping mode of the *PHS* plant in the year 2022. The correspondence between these two figures can be seen when comparing Figures 8 and 11.
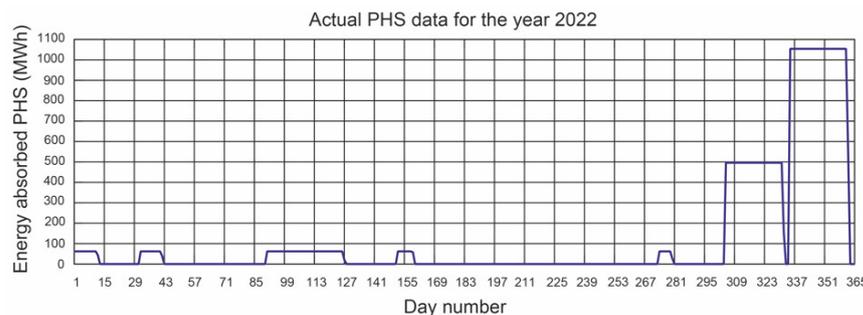

Figure 11. Daily energy absorbed by the PHS plant during the year 2022.

The annual energy absorbed in pumping mode was 47.09 (GWh). Therefore, in 2022, this plant absorbed more energy than it generated: specifically, 28.49 (GWh).

From an economic point of view, the cost of this absorbed energy was EUR 5,047,474.74. It can be concluded that this *PHS* plant operated under economic losses during the year 2022.

4.4. Operation of the PHS Plant Together with the FPV Plant

Figure 12 shows the energy generated by the analysed *FPV* plants. Figure 12a shows the hourly distribution of the energy generated by the *FPV* plant size *S2* on 21 June (Summer Solstice). Figure 12b shows the daily distribution of the energy generated by each *FPV* plant size.
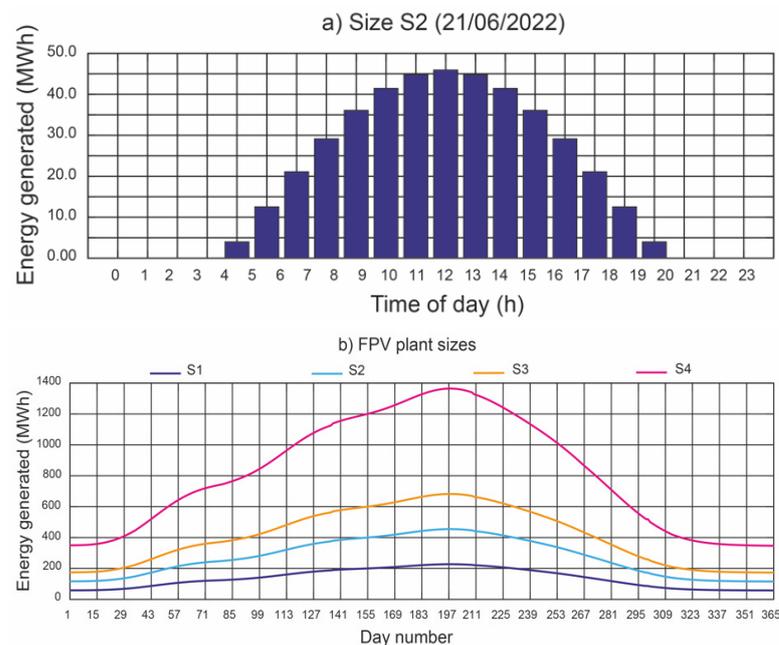
Figure 12. Energy generated by the sizes of FPV plants analysed.

4.4.1. 4 h of Daily *PHS* Plant Operation

Figure 13 shows the daily energy generated with 4 h daily *PHS* plant operation during the year 2022, using the water pumped with the energy generated by each size of the *FPV* plant, i.e., joint operation mode of both plants. With the *FPV* plant size *S1*, the *PHS* plant is not operational every day of the year. In contrast, the *PHS* plant is operational every day of the year with the other sizes. In addition, water storage is achieved in the upper reservoir, namely 12.28% and 51.21%, respectively, with the *FPV* plant sizes *S3* and *S4*. The *PHS* plant operates under Case 1 conditions: No deviation. In addition, it operates during the 4 h of highest electricity market prices.

Figure 14 shows the economic benefit from the independent and joint operation modes of both plants, for the sizes *S1* and *S2* and pumping process efficiency of 0.77 and 0.85.

The joint operation mode is characterised by 4 h of *PHS* plant operation per day during the year 2022, using the water pumped with the energy generated by the *FPV* plant sizes *S1* and *S2*.

The independent operation mode is characterised by 4 h of daily *PHS* plant operation during the year 2022 depending on the available water and *FPV* plant sizes selling the energy as it is generated. The *FPV* plant operates under Case 1 conditions: No deviation.

For $\mu = 0.77$, the economic benefit is always higher in the independent mode of operation. This is true even if there are deviations of 10%, in Cases 3 and 4.
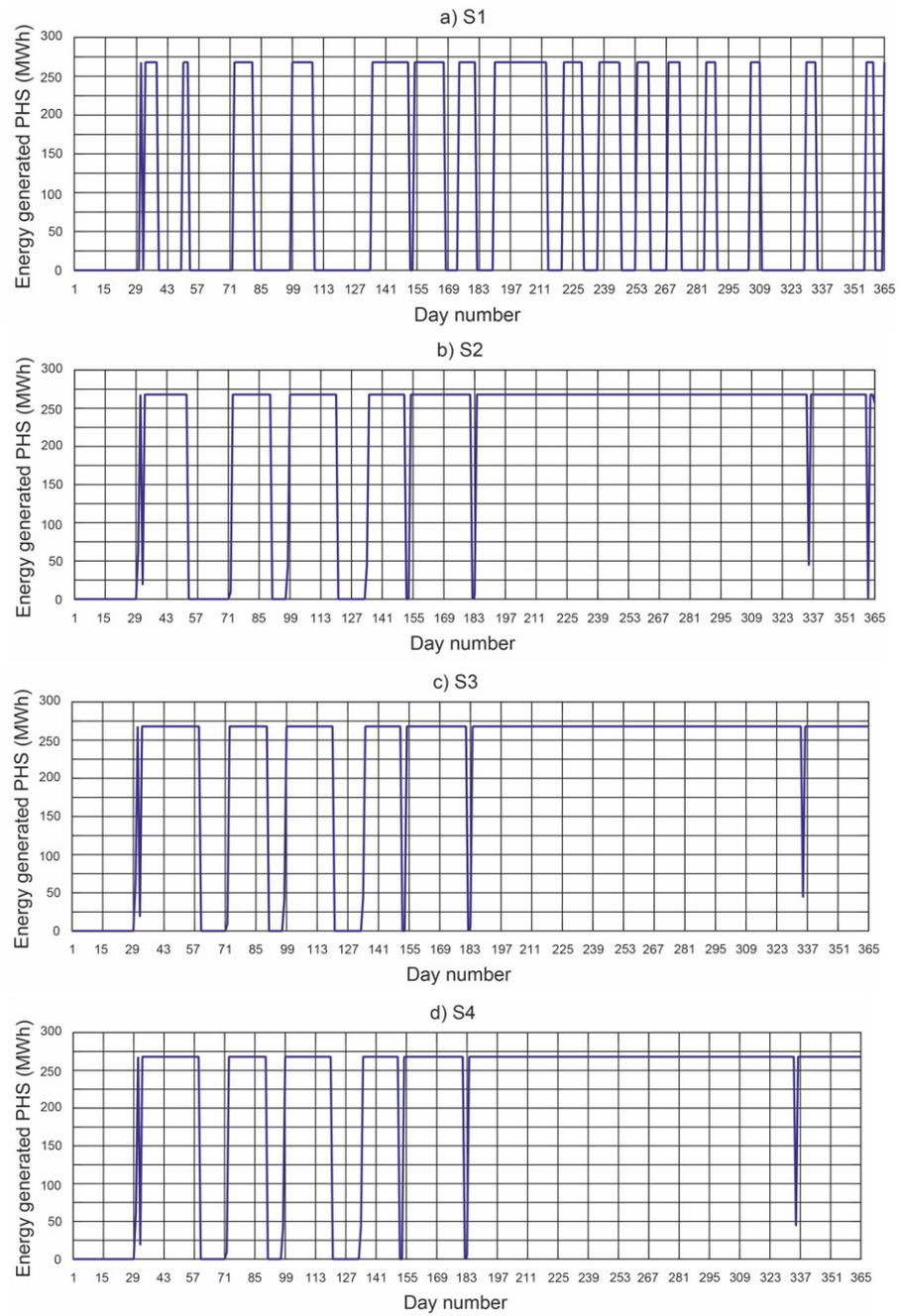
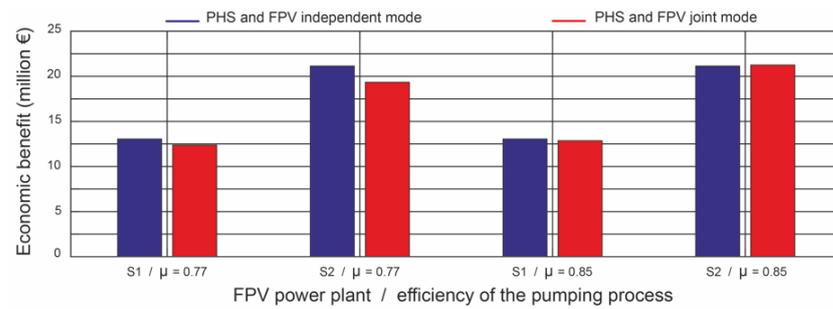**Figure 13.** Daily energy generated by the PHS plant during the year 2022.
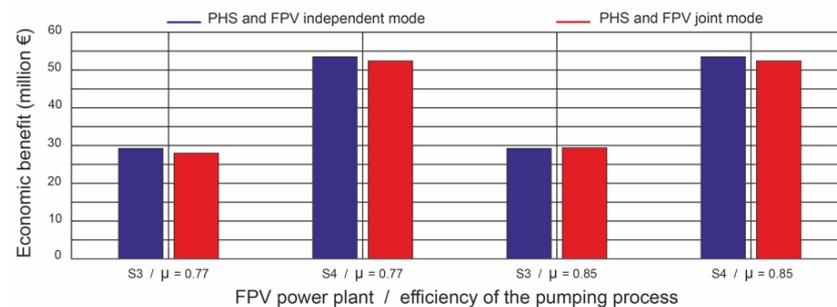

Figure 14. Economic benefit from the independent and joint operation modes with S1 and S2.

For $\mu = 0.85$, the economic benefit is slightly higher in the joint operation mode of *FPV* plant size *S2*. If the *FPV* plant size is *S1*, the economic benefit is slightly higher in the independent operation mode. However, if deviations of 10% occur in Cases 3 and 4, the economic benefit is slightly higher in the joint operation mode.

Figure 15 shows the economic benefit from the independent and joint operation modes of both plants, for the sizes *S3* and *S4* and the pumping process efficiency of 0.77 and 0.85.

Figure 15. Economic benefit of the independent and joint operation modes with *S3* y *S4*.

The joint operation mode is characterised by 4 h of daily *PHS* plant operation during the year 2022, using the water pumped with the energy generated by the *FPV* plant sizes *S3* and *S4*. The surplus energy from the *FPV* plant is sold as it is generated. The *FPV* plant operates under Case 1 conditions: No deviation.

The independent operation mode is characterised by 4 h daily *PHS* plant operation during the year 2022 depending on the available water and *FPV* plant sizes selling the energy as it is generated. The *FPV* plant operates under Case 1 conditions: No deviation.

For $\mu = 0.77$, the economic benefit is always higher in the independent mode of operation. This is true even if there are deviations of 10%, in Cases 3 and 4.

For $\mu = 0.85$, the economic benefit is slightly higher in the joint operation mode of the *FPV* plant size *S3*. If the *FPV* plant size is *S4*, the economic benefit is slightly higher in the independent operation mode. This is true even if there are deviations of 10%, in Cases 3 and 4.

The more important renewable energies become in the electricity market, the greater the need for an energy storage system. Therefore, as the results obtained here are very similar in the joint and independent operation mode of both plants, it can be assumed that the economic benefit from the joint operation mode of both plants will increase as the need for energy storage increases. Several studies confirm that the joint operation mode of both plants can play an important role in balancing systems with a high penetration of variable renewables [26].

4.4.2. 5 or More Daily Hours of *PHS* Plant Operation

Figure 16 shows the economic benefit from the independent and joint operation modes of both plants for the size *S4* with the pumping process efficiencies of 0.77 and 0.85, and 5 daily hours of *PHS* plant operation.

The joint operation mode is characterised by 5 h per day of *PHS* plant operation during the year 2022, using the water pumped with the energy generated by the *FPV* plant size *S4* and when the surplus energy from the *FPV* plant is sold as it is generated. The *FPV* plant operates under Case 1 conditions: No deviation.

The independent operation mode is characterised by 4 h of daily *PHS* plant operation during the year 2022 depending on the available water and *FPV* plant selling the energy as it is generated. The *FPV* plant operates under Case 1 conditions: No deviation.

For $\mu = 0.77$ and $\mu = 0.85$, the economic benefit is always higher in the independent mode of operation. This is true even if there are deviations of 10% in Cases 3 and 4.

For all other plant sizes, the economic benefit is always higher in the independent mode of operation. This profit increases as the power of the *FPV* plant decreases.
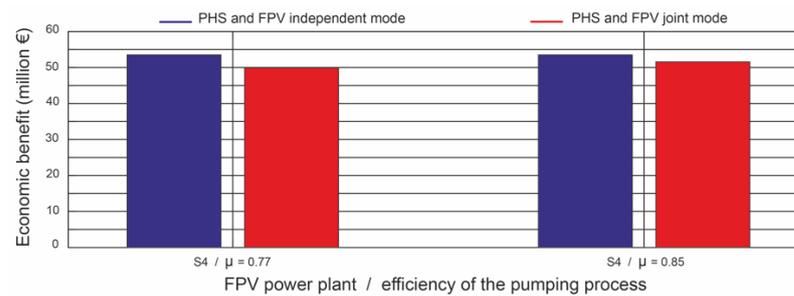
Figure 16. Economic benefit from the independent and joint operation modes with S4.

5. Conclusions

This paper examines the sizing of a floating photovoltaic (*FPV*) power plant for integration into an existing pumped hydroelectric storage (*PHS*) power plant in order to improve the performance thereof. In addition, the parameter known *PHS* plant total process efficiency is also used to evaluate the plant. The Alto Rabagão pumped hydroelectric storage power plant in Northern Portugal was the subject of the study. The following power outputs were analysed for the *FPV* plant: 33.55 (*MWp*) (50% *PHS*), 67.1 (*MWp*) (100% *PHS*), 100.65 (*MWp*) (150% *PHS*), 201.30 (*MWp*) (300% *PHS*), and 301.95 (*MWp*) (450% *PHS*). These *FPV* plant sizes are referred to as *S*1, *S*2, *S*3, *S*4 and *S*5, respectively. The values of the total process efficiency parameter analysed are 0.77 for old *PHS* plants, and 0.85 for more modern plants. The results obtained confirm which scenarios earn economic benefits from a *PHS* plant and an *FPV* plant operating together or independently.

The study shows the following conclusions regarding the volume of water in the upper reservoir:

(i) The actual data showed that the volume of water available in the upper reservoir is a critical parameter that determines the *PHS* plant operating days. The *PHS* plant only operated 20% of the days in 2022. In addition, more energy is absorbed in the pumping process than the energy generated by the *PHS* plant. Therefore, the economic benefit was negative.

(ii) The sizes of the *FPV* plants analysed occupy a very small body of water compared to the total surface area of the upper reservoir, specifically, 1.018% for *S*1, 2.04% for *S*2, 3.05% for *S*3, 6.12% for *S*4, and 9.16% for *S*5.

(iii) The *FPV* plant sizes analysed have the capacity to reach significant higher reservoir levels (if all the energy generated by the *FPV* plant sizes was used to pump water), specifically, 16.85% for *S*1, 33.71% for *S*2, 50.56% for *S*3, 101.13% for *S*4 and 151.69% for *S*5.

(iv) In total, 100% of the water volume of the upper reservoir is obtained with an occupied water body surface of 6.12%.

From an economic benefit point of view and taking into account 4 h of *PHS* plant operation per day during the year 2022 (the 4 h of highest electricity market prices and the *PHS* plant always operating under the conditions of Case 1: No deviation), the study shows the following conclusions:

(i) During joint operation of both plants, the *S*1 size *FPV* plant is not able to operate the *PHS* plant every day of the year. In addition, the economic benefit is slightly higher with the independent operation mode (Case 1: No deviations), regardless of the value of the total process efficiency parameter analysed. However, if deviations of 10% occur in Cases 3 and 4, the economic benefit is slightly higher in the joint operation mode.

(ii) During the joint operation of both plants, the *S*2 size of the *FPV* plant is able to operate the *PHS* plant every day of the year. If the total process efficiency is 0.85, this mode of operation earns a slightly higher economic benefit than the independent operation of both plants (Case 1: No deviations).

(iii) During joint operation of both plants, the *FPV* plant sizes *S3* and *S4* are able to operate the *PHS* plant every day of the year and, in addition, obtain a surplus water volume of 12.28% and 51.21%, respectively, of the capacity of the upper reservoir.

(iv) During joint operation of both plants, the *S3* size of *FPV* plant is able to operate the *PHS* plant every day of the year and sell the surplus energy directly as it is generated (in this case, no water is stored). If the total process efficiency is 0.85, this mode of operation earns a slightly higher economic benefit than the independent operation mode of both plants (Case 1: No deviations).

(v) In the joint operation of both plants, the *FPV* plant size *S4* is able to operate the *PHS* plant every day of the year and sell the surplus energy directly as it is generated (in this case, no water is stored). The economic benefit is slightly higher with the independent operation mode (Case 1: No deviations), regardless of the value of the total process efficiency parameter analysed.

In summary, if the total process efficiency is 0.85, the joint operation of both plants with *FPV* plant sizes *S2* and *S3* yields a slightly higher economic benefit than the independent mode of operation. If the total process efficiency is 0.77, there is always a higher economic benefit in the independent operation mode, irrespective of the size of the *FPV* plant. However, the uncertainty of the solar resource estimation can lead to a higher economic benefit in the joint operation mode.

Increasing the number of *PHS* plant operating hours above 4 h per day decreases the economic benefit from the joint operation mode, regardless of the total process efficiency parameter and the size of the *FPV* plant. The economic benefit decreases as the number of operating hours increases.

Nomenclature

A_T	Total surface area of the *PV* modules (m^2)
E_{PV}	Total energy (Wh)
g	Acceleration due to gravity (m/s^2)
H_t	Total irradiation on a tilted surface (Wh/m^2)
h_a	Available head (m)
h_e	Elevating head (m)
I_{bh}	Beam irradiance on a horizontal surface (W/m^2)
I_{dh}	Diffuse irradiance on a horizontal surface (W/m^2)
I_t	Total irradiance on a tilted surface (W/m^2)
k_p	Water pumping coefficient (W· s/m^3)
k_t	Turbine generating coefficient (W· s/m^3)
L_{PV}	Module PV length (m)
$NOCT$	Normal operating cell temperature (°)
n	Ordinal of the day (day)
P_a	Power input of the electric motor (W)
P_g	Power output of the electric generator (W)
P_{PV}	Power output of the *PV* module (W/m^2)
P_t	Power output of the hydro turbine (W)
q_t	Turbined flow rate (m^3/s)
q_p	Pumped flow rate (m^3/s)

T	Solar time (h)
T_a	Ambient temperature (°)
T_c	*PV* cell temperature (°C)
T_{ref}	Reference temperature (°C)
T_R	Sunrise solar time (h)
T_S	Sunset solar time (h)
W_{PV}	Module PV width (m)
α	Solar absorptance of *PV* layer (dimensionless)
β	Tilt angle of photovoltaic module (°)
β_{ref}	Temperature coefficient (1/°C)
γ	Azimuth angle of photovoltaic module (°)
δ	Solar declination (°)
η_e	PV module efficiency (%)
η_g	Electric generator efficiency (%)
η_m	Motor generator efficiency (%)
η_p	Pump efficiency (%)
η_{ref}	*PV* module efficiency at the reference temperature (%)
η_t	Hydro turbine efficiency (%)
θ_i	Incidence angle (°)
θ_z	Zenith angle of the Sun (°)
λ	Latitude angle (°)
μ	Total pumping process efficiency (%)
ρ	Density of water (kg/m^3)
ρ_g	Ground reflectance (dimensionless)
τ	Solar transmittance of glazing (dimensionless)
ω	Hour angle (°)

References

1. The Paris Agreement. Paris Agreement. In Proceedings of the Conference of the Parties to the United Nations Framework Convention on Climate Change (21st Session), Paris, France, 30 November–13 December 2015.
2. Bouckaert, S.; Pales, A.F.; McGlade, C.; Remme, U.; Wanner, B.; Varro, L.; D'Ambrosio, D.; Spencer, T.; Abergel, T.; Arsalane, Y.; et al. Net Zero by 2050: A Roadmap for the Global Energy Sector. International Energy Agency (IEA). 2021. Available online: https://www.iea.org/reports/net-zero-by-2050 (accessed on 10 April 2023).
3. BPIE. 9 Ways to Make the Energy Performance of Buildings Directive More Effective. 2016. Available online: http://bpie.eu/wp-content/uploads/2016/08/EPBD-paper_Eng.pdf (accessed on 27 January 2023).
4. BP Statistical Review of World Energy. 2021. Available online: https://www.bp.com/content/dam/bp/business-sites/en/global/corporate/pdfs/energy-economics/statistical-review/bp-stats-review-2021-full-report.pdf (accessed on 27 January 2023).
5. Barbón, A.; Fortuny Ayuso, P.; Bayón, L.; Silva, C.A. A comparative study between racking systems for photovoltaic power systems. *Renew. Energy* **2021**, *180*, 424–437. [CrossRef]
6. Lin, F.; Zhang, Y.; Wang, J. Recent advances in intra-hour solar forecasting: A review of ground-based sky image methods. *Int. Forecast.* **2023**, *39*, 244–265. [CrossRef]
7. U.S. Department of Energy, Energy Efficiency and Renewable Energy. Types of Hydropower Plants. 2023. Available online: https://www.energy.gov/eere/water/types-hydropower-plants (accessed on 10 April 2023).
8. Agrawal, K.K.; Jha, S.K.; Mittal, R.K.; Vashishtha, S. Assessment of floating solar PV (FSPV) potential and water conservation: Case study on Rajghat Dam in Uttar Pradesh, India. *Energy Sustain. Dev.* **2022**, *66*, 287–295. [CrossRef]
9. Sanseverino, I.; Conduto, D.; Pozzoli, L.; Dobricic, S., Lettieri, T. Algal Bloom and Its Economic Impact, European Commission, Joint Research Centre. 2016. Available online: https://op.europa.eu/en/publication-detail/-/publication/4d384d1b-1804-11e6-ba9a-01aa75ed71a1/language-en (accessed on 10 April 2023).
10. Muñoz-Cerón, E.; Osorio-Aravena, J.C.; Rodríguez-Segura, F.J.; Frolova, M.; Ruano-Quesada, A. Floating photovoltaics systems on water irrigation ponds: Technical potential and multi-benefits analysis. *Energy* **2023**, *271*, 127039. [CrossRef]
11. Nguyen, N.H.; Le, B.C.; Nguyen, L.N.; Bui, T.T. Technical analysis of the large capacity grid-connected floating photovoltaic system on the hydropower reservoir. *Energies* **2023**, *16*, 3780. [CrossRef]
12. Al-Widyan, M.; Khasawneh, M.; Abu-Dalo, M. Potential of floating photovoltaic technology and their effects on energy output, water quality and supply in Jordan. *Energies* **2021**, *14*, 8417. [CrossRef]
13. Padilha Campos Lopes, M.; Nogueira, T.; Leandro Santos, A.J.; Castelo Branco, D.; Pouran, H. Technical potential of floating photovoltaic systems on artificial water bodies in Brazil. *Renew. Energy* **2022**, *181*, 1023–1033. [CrossRef]
14. Martín-Chivelet, N. Photovoltaic potential and land-use estimation methodology. *Energy* **2016**, *94*, 233–242. [CrossRef]
15. El Hammoumi, A.; Chalh, V.; Allouhi, A.; Motahhir, S.; El Ghzizal, A.; Derouich, A. Design and construction of a test bench to investigate the potential of floating PV systems. *J. Clean. Prod.* **2021**, *278*, 123917. [CrossRef]

16. Liu, H.; Krishna, V.; Lun Leung, J.; Reindl, T.; Zhao, L. Field experience and performance analysis of floating PV technologies in the tropics. *Prog. Photovolta. Res. Appl.* **2018**, *26*, 957–967. [CrossRef]

17. Cramton, P. Electricity market design. *Oxf. Rev. Econ. Policy* **2017**, *33*, 589–612. [CrossRef]

18. Barbón, A.; Gutiérrez, A.; Bayón, L.; Bayón-Cueli, C.; Aparicio-Bermejo, J. Economic analysis of a pumped hydroelectric storage-integrated floating PV system in the day-ahead Iberian electricity market. *Energies* **2023**, *16*, 1705. [CrossRef]

19. Jurasz, J.; Canales, F.A.; Kies, A.; Guezgouz, M.; Beluco, A. A review on the complementarity of renewable energy sources: concept, metrics, application and future research directions. *Sol. Energy* **2020**, *195*, 703–724. [CrossRef]

20. Kougias, I.; Szabó, S. Pumped hydroelectric storage utilization assessment: Forerunner of renewable energy integration or Trojan horse? *Energy* **2017**, *140*, 318–329. [CrossRef]

21. Rehman, S.; Al-Hadhrami, L.M.; Alam, M.M. Pumped hydro energy storage system: A technological review. *Renew. Sustain. Rev.* **2015**, *44*, 586–598. [CrossRef]

22. Margeta, J.; Glasnovic, Z. Theoretical settings of photovoltaic-hydro energy system for sustainable energy production. *Solar Energy* **2012**, *86*, 972–982. [CrossRef]

23. Rauf, H.; Gull, M.S.; Arshad, N. Complementing hydroelectric power with floating solar PV for daytime peak electricity demand. *Renew. Energy* **2020**, *162*, 1227–1242. [CrossRef]

24. Kocaman, A.S.; Modi, V. Value of pumped hydro storage in a hybrid energy generation and allocation system. *Appl. Energy* **2017**, *205*, 1202–1215. [CrossRef]

25. Glasnovic, Z.; Margeta, J. The features of sustainable solar hydroelectric power plant. *Renew. Energy* **2009**, *34*, 1742–1751. [CrossRef]

26. Bhattacharjee, S.; NayakP.K. PV-pumped energy storage option for convalescing performance of hydroelectric station under declining precipitation trend. *Renew. Energy* **2019**, *135*, 288–302. [CrossRef]

27. Ciucci, M. Internal Energy Market, Fact Sheets on the European Union. 2022. Available online: https://www.europarl.europa.eu/factsheets/en/sheet/45/internal-energy-market (accessed on 27 January 2023).

28. EDP. Available online: https://portugal.edp.com/en/alto-rabagao-hydro-power-plant (accessed on 27 December 2022).

29. Bayón, L.; Grau, J.M.; Ruiz, M.M.; Suárez, P.M. Mathematical modelling of the combined optimization of a pumped-storage hydro-plant and a wind park. *Math. Comput. Model.* **2013**, *57*, 2024–2028. [CrossRef]

30. Ibrahim, H.; Ilinca, A.; Perron, J. Energy storage systems–characteristics and comparisons. *Renew. Sustain. Energy Rev.* **2008**, *12*, 1221–1250. [CrossRef]

31. Khalil Zidane, T.E.; Bin Adzman, M.R.; Naim Tajuddin, M.F.; Mat Zali, S.; Durusu, A. Optimal configuration of photovoltaic power plant using grey wolf optimizer: A comparative analysis considering CdTe and c-Si PV modules. *Sol. Energy* **2019**, *188*, 247–257. [CrossRef]

32. Kalogirou, S.A.; Agathokleous, R.; Panayiotou, G. On-site PV characterization and effect of soiling on their performance. *Energy* **2013**, *51*, 439–446. [CrossRef]

33. Skoplaki, E.; Palyvos, J.A. On the temperature dependence of photovoltaic module electrical performance: A review of efficiency/power correlations. *Sol. Energy* **2009**, *83*, 614–624. [CrossRef]

34. Evans, D.L. Simplified method for predicting photovoltaic array output. *Sol. Energy* **1981**, *27*, 555–560. [CrossRef]

35. Kichou, S.; Skandalos, N.; Wolf, P. Floating photovoltaics performance simulation approach. *Heliyon* **2022**, *8*, 11896. [CrossRef] [PubMed]

36. Lawrence Kamuyu, W.C.; Rok Lim, J.; Sub Won, C.; Keun Ahn, H. Prediction model of photovoltaic module temperature for power performance of floating PVs. *Energies* **2018**, *11*, 447. [CrossRef]

37. Dutra Silva, D.; Marson, V.; Rodrigues de Souza, R.; Diehl de Oliveira, J.; Campos Silva, J.B.; Cardoso, E.M. A new predictive model for a photovoltaic module's surface temperature. *Energy Rep.* **2022**, *8*, 15206–15220. [CrossRef]

38. Skoplaki, E.; Palyvos, J.A. Operating temperature of photovoltaic modules: A survey of pertinent correlations. *Renew. Energy* **2009**, *34*, 23–29. [CrossRef]

39. Mattei, M.; Notton, G.; Cristofari, C.; Muselli, M.; Poggi, P. Calculation of the polycrystalline PV module temperature using a simple method of energy balance. *Renew. Energy* **2006**, *31*, 553–567. [CrossRef]

40. Choi, Y.K. A study on power generation analysis of floating PV system considering environmental impact. *Int. J. Softw. Eng. Appl.* **2014**, *8*, 75–84. [CrossRef]

41. Oliveira-Pinto, S.; Stokkermans, J. Assessment of the potential of different floating solar technologies–Overview and analysis of different case studies. *Energy Convers. Manag.* **2020**, *211*, 112747. [CrossRef]

42. Duffie, J.A.; Beckman, W.A. *Solar Engineering of Thermal Processes*, 4th ed.; John Wiley & Sons: New York, NY, USA, 2013.

43. Barbón, A.; Fortuny Ayuso, P.; Bayón, L.; Fernández-Rubiera, J.A. Predicting beam and diffuse horizontal irradiance using Fourier expansions. *Renew. Energy* **2020**, *154*, 46–57. [CrossRef]

44. WRDC. World Radiation Data Centre. 2022. Available online: http://wrdc.mgo.rssi.ru/ (accessed on 27 January 2023).

45. Bhavani, S.; Chithambaram, V.; Muthucumaraswamy, R.; Shanmugan, S.; Essa, F.A.; Elsheikh, A.H.; Selvaraju, P.; Janarthanan, B. Laplacian tactic for the prediction of the temperature components of solar cooker with logical prediction by fuzzy rules. *Sol. Energy* **2022**, *236*, 369–382. [CrossRef]

46. Barbón, A.; Bayón-Cueli, C.; Bayón, L.; Carreira-Fontao, V. A methodology for an optimal design of ground-mounted photovoltaic power plants. *Appl. Energy* **2022**, *314*, 118881. [CrossRef]

47. Hottel, H.C. A simple model for estimating the transmittance of direct solar radiation through clear atmosphere. *Sol. Energy* **1976**, *18*, 129–134. [CrossRef]
48. Liu, B.Y.H.; Jordan, R.C. The interrelationship and characteristic distribution of direct, diffuse and total solar radiation. *Sol. Energy* **1960**, *4*, 1–19. [CrossRef]
49. PVGIS, Joint Research Centre (JRC). 2022. Available online: http://re.jrc.ec.europa.eu/pvg_tools/en/tools.html#PVP (accessed on 27 January 2023).
50. Ghigo, A.; Faraggiana, E.; Sirigu, M.; Mattiazzo, G.; Bracco, G. Design and analysis of a floating photovoltaic system for offshore installation: The case study of Lampedusa. *Energies* **2022**, *15*, 8804. [CrossRef]
51. Bayón-Cueli, C.; Barbón, A.; Fernández-Conde, A.; Bayón, L. Optimal distribution of PV modules on roofs with limited space. In Proceedings of the 2021 IEEE International Conference on Environmental and Electrical Engineering (EEEIC2021), Bari, Italy, 7–10 September 2021; pp. 50–55.
52. Isifloating. Available online: https://www.isifloating.com/en/solar-flotante-isifloating-by-isigenere-english/ (accessed on 27 January 2023).
53. Osborne, M. Sungrow Targets Teading Role in Supply of Floating Solar Systems to Booming Market. Available online: https://www.pv-tech.org/sungrow-targets-leading-role-in-supply-of-floating-solar-systems-to-booming/ (accessed on 10 April 2023).
54. Sahu, A.; Yadav, N.; Sudhakar, K. Floating photovoltaic power plant: A review. *Renew. Sustain. Energy Rev.* **2016**, *66*, 815–824. [CrossRef]
55. Ciel. Available online: https://ciel-et-terre.net/solutions/products/ (accessed on 27 January 2023).
56. Intech. Available online: https://intechcleanenergy.com/floating-panels.php (accessed on 27 January 2023).
57. Muneer, T. *Solar Radiation and Day Light Models*, 1st ed.; Elsevier: Oxford, UK, 2004.
58. Dobos, E. Albedo. *Encycl. Soil Sci.* **2006**, *2*, 24–25.
59. Weihs, P.; Mursch-Radlgruber, E.; Hasel, S.; Gützer, C.; Brandmaier, M.; Plaikner, M. Investigation of the effect of sealed surfaces on local climate and thermal stress. In *EGU General Assembly Conference Abstracts*; Copernicus GmbH: Göttingen, Germany, 2015; p. 12616.
60. Pérez-Gallardo, J.R.; Azzaro-Pantel, C.; Astier, S.; Domenech, S.; Aguilar-Lasserre, A. Ecodesign of photovoltaic grid-connected systems. *Renew. Energy* **2014**, *64*, 82–97. [CrossRef]
61. ESIOS, 2023; Iberian Market Operator, Market Results. Available online: https://www.esios.ree.es/es/mercados-y-precios (accessed on 27 January 2023).
62. SNIRH. 2023. Available online: https://snirh.apambiente.pt/index.php?idMain=1&idItem=1.3&sbaciaid=&szonas=&salbufeirasimbolo=03J/03A&n_mesBOLETIM=01&n_anoH= (accessed on 27 January 2023).